View metadata, citation and similar papers at core.ac.uk

brought to you by CORE

provided by Purdue E-Pubs

Purdue University
Purdue e-Pubs

International Refrigeration and Air Conditioning Conference

School of Mechanical Engineering

2012

Simulation-Based Design and Optimization of Frost-Free Refrigerators: A Thermoeconomic Approach

Rodrigo Mitishita
chermes@ufpr.br

Eduardo Barreira

Cezar Negrao

Christian Hermes

Follow this and additional works at: http://docs.lib.purdue.edu/iracc

Mitishita, Rodrigo; Barreira, Eduardo; Negrao, Cezar; and Hermes, Christian, "Simulation-Based Design and Optimization of Frost-Free Refrigerators: A Thermoeconomic Approach" (2012). *International Refrigeration and Air Conditioning Conference.* Paper 1163.
http://docs.lib.purdue.edu/iracc/1163

This document has been made available through Purdue e-Pubs, a service of the Purdue University Libraries. Please contact epubs@purdue.edu for additional information.
Complete proceedings may be acquired in print and on CD-ROM directly from the Ray W. Herrick Laboratories at https://engineering.purdue.edu/Herrick/Events/orderlit.html

Simulation-Based Design and Optimization of Frost-Free Refrigerators: A Thermoeconomic Approach

Rodrigo S. MITISHITA [1], Eduardo M. BARREIRA [1], Cezar O. R. NEGRÃO [1], Christian J. L. HERMES [2,*]

[1] Thermal Science Laboratory, Postgraduate Program of Mechanical and Materials Engineering, Federal University of Technology – Paraná, Av. Sete de Setembro 3165, 80230901 Curitiba-PR, Brazil

[2] Center for Applied Thermodynamics, Department of Mechanical Engineering, Federal University of Paraná P.O. Box 19011, 81531990 Curitiba-PR, Brazil

[*] Corresponding author: chermes@ufpr.br, +55-41-3361-3239

ABSTRACT

A steady-state simulation model was devised and its predictions for energy consumption were compared with experimental data obtained elsewhere, with differences not exceeding a 9% error band. The model was used to find out the evaporator air flow rate, the number of evaporator and condenser fins, the compressor size and efficiency, and the insulation thicknesses of both compartments which yield the minimum energy consumption when the total cost is constrained. The optimization led to a refrigeration system with energy consumption 18% lower than that observed for the baseline system without any cost penalty. The system performance for four different compressors including a high efficiency, a large capacity and a variable-speed one was also analyzed. According to the cost function adopted, the variable-speed compressor shall not cost 26% more than a single-speed one with the same piston displacement.

1. INTRODUCTION

Frost-free refrigerators are small-capacity (~100 W) refrigerating appliances comprised of one or more polyurethane insulated compartments and, in most cases, of a vapor compression refrigeration loop running with HFC134a or HC600a. The task of developing new household refrigerators is motivated not only for energy consumption regulations and environmental issues (Melo and Silva, 2010), but also for the pursuit of more profitable products (Negrão and Hermes, 2011). In general, frost-free refrigerators are designed following a trial-and-error component matching approach based on costly and time demanding standardized test procedures, which may turn the development of new refrigerators an expensive endeavor (Hermes et al., 2012). It has been advocated in the open literature that the costs associated with the development of household refrigerators may be reduced dramatically if proper system simulation tools are adopted (Hermes and Melo, 2008; Gonçalves et al., 2009; Hermes et al., 2009; Borges et al., 2011), which have to predict not only the overall energy consumption accurately, but also the total system cost. Nevertheless, cost reduction and energy savings are tradeoff design criteria (Negrão and Hermes, 2011), in such a way that there does exist a minimum cost for a target energy consumption and vice-versa.

Optimization methods can be used together with system simulation tools in order to obtain the minimum energy consumption for a given cost. In general, the methods available in the open literature consider a single component at a time, without any cost concerns (Bansal and Chin, 2003; Gholap and Khan, 2007; Waltrich et al., 2011a). Indeed, just a few studies of cost and energy optimization for the entire refrigeration system can be found. For instance, Waltrich et al. (2011b) presented a model-based methodology to optimize the energy and cost of a refrigeration cassette for light commercial applications by changing not only the condenser and evaporator characteristics but also the compressor size. The optimization came out with an improved cassette design with a COP/cost ratio by 50% higher than that of the baseline system. Negrão and Hermes (2011) proposed an optimization approach for a household vertical freezer considering the heat transfer areas of the natural draft condenser and evaporator, the cabinet insulation thickness, and the compressor size and efficiency as optimization parameters. The results showed either cost reductions of 6% for a fixed energy consumption or energy savings of 14% for a fixed cost.

Nonetheless, it has not been found in the open literature an optimization methodology applicable to frost-free refrigerators, a kind of household refrigerating appliance whose features include a particular type of fan-supplied tube-fin evaporator, and two insulated compartments (at least) usually at -18°C and 5°C for frozen and fresh-food storage, respectively. The present paper is, therefore, aimed at developing and validating a multi-parameter (i.e., evaporator and condenser finned areas, insulation thicknesses of both the frozen and fresh-food compartments, compressor type, size and efficiency, and evaporator air flow rate) simulation-based optimization approach for frost-free refrigerators focused on both energy and cost savings. The optimization algorithm was also employed to figure out how economically feasible is the application of a variable-speed compressor to a particular refrigeration system.

2. SIMULATION MODEL

The object of this study is a 440-liter frost-free refrigerator designed for the Brazilian market and comprised of a hermetic single-speed compressor running with HFC-134a as a working fluid and ISO-10 POE oil, a natural draft wire-and-tube condenser with 90 wires, a fan-supplied tube-fin evaporator with 27 flat fins distributed unevenly along the coil, a concentric tube-in-tube counterflow heat exchanger formed by inserting the capillary tube into the suction line, and two insulated compartments made of 65-mm (frozen-food) and 47-mm (fresh-food) thick polyurethane foam. The simulation model was devised assuming that the refrigeration system operates at steady-state regime, whereas the effect of the *on* and *off* cycles induced by the thermostat was taken into account by a compressor runtime ratio obtained from an overall energy balance over a full compressor cycle (Hermes et al., 2009). Thus, component-level models following a lumped approach were developed based on mass and energy balances for each of the following components: compressor, condenser, capillary tube suction line heat exchanger, evaporator and refrigerated compartments.

It is well-known from the open literature (Hermes and Melo, 2008; Hermes et al., 2009; Negrão and Hermes, 2011) that there are two important issues that are quite difficult to handle in refrigeration system modeling: the non-adiabatic expansion through the capillary tube and the refrigerant charge inventory. The compressible two-phase diabatic flow through a small-bore tube is complex and its modeling usually demands significant computational effort (Hermes et al., 2008), while the prediction of mass distribution within the system is cumbersome because of the non-homogeneous two-phase flow in condensers and evaporators (Rice, 1987). Therefore, it was assumed that the outlet conditions of the evaporator and condenser are known, i.e. the superheating and sub-cooling degrees were prescribed for the evaporator and the condenser, respectively, in such a way that the outlet evaporator and condenser temperatures can be calculated straightforwardly from $T_e=T_{sat}(p_e)=T_5-\Delta T_{sh}$ and $T_c=T_{sat}(p_c)=T_3+\Delta T_{sc}$, respectively, where p_c is the condensing pressure, p_e is the evaporating pressure, and points 3 and 5 are depicted in the schematic representation of the refrigeration system (see Fig. 1). This approach not only eliminates potential convergence issues, but also narrows the gap between the numerical analysis and the design practice of adjusting the refrigerant charge and the capillary tube size (bore and length) afterwards in order to obtain the desired degree of evaporator superheating and condenser subcooling (Hermes et al., 2009; Negrão and Hermes, 2011).

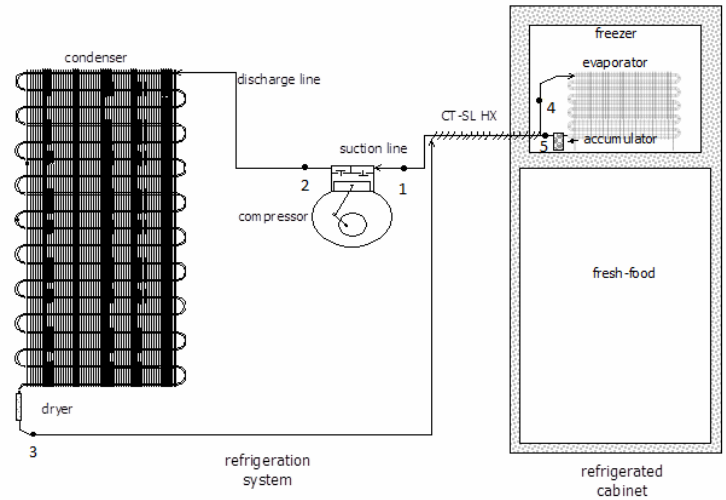

Figure 1. Schematic representation of the refrigeration system (Hermes and Melo, 2008)

2.1 Condenser and Evaporator

Following a lumped modeling approach, the heat released by the condenser, Q_c, can be calculated from:

$$Q_c = UA_c(T_c - T_a) = m_r(h_2 - h_3) \quad (1)$$

where T_c is the condensing temperature, T_a is the ambient temperature, m_r is the refrigerant mass flow rate, and UA_c is the thermal conductance of the condenser. The subscripts 2 and 3 refer to the refrigerant at the condenser inlet and outlet, respectively (see Fig. 1). Similarly, the heat absorbed by the evaporator is calculated as follows:

$$Q_e = m_{air} c_{p,air}(T_m - T_e)\left(1 - \exp\left(-UA_e / m_{air} c_{p,air}\right)\right) = m_r(h_5 - h_4) \quad (2)$$

where m_{air} is the air flow rate supplied to the evaporator by the fan, $c_{p,air}$ is the specific heat of the air stream calculated at the inlet temperature, UA_e is the thermal conductance of the evaporator, and the subscripts 4 and 5 refer to the evaporator inlet and outlet, respectively. In addition, T_e is the evaporating temperature, $T_m=\phi T_{fz}+(1-\phi)T_{ff}$ is the mean air temperature at the evaporator inlet, where ϕ is the fraction of air flow rate supplied to the frozen-food compartment, and T_{ff} and T_{fz} are the fresh- and frozen-food compartment temperatures, respectively.

2.2 Capillary Tube Suction Line Heat Exchanger

An overall energy balance in the heat exchanger formed by the capillary tube and the suction line provides an equation for the refrigerant enthalpy at the evaporator inlet, $h_4=h_3-h_1+h_5$, where the heat transfer to the surrounding air was neglected. The refrigerant flow through the capillary tube can be divided into two domains namely, liquid and two-phase regions. It should be noted that the refrigerant temperature within the capillary tube changes not only because of the heat loss in the liquid region but also because of the pressure drop in the two-phase flow region (Hermes et al., 2008). However, for the sake of heat transfer calculations, the capillary tube can be assumed to be filled with liquid refrigerant and, therefore, the concept of heat exchanger effectiveness can be used to calculate the refrigerant temperature at the compressor inlet, $T_1=\varepsilon T_3+(1-\varepsilon)T_5$, where ε is the effectiveness of the counterflow tube-in-tube heat exchanger.

2.3 Compressor

An overall energy balance applied to the compressor shell yields,

$$W_k = m_r(h_2 - h_1) + UA_k(T_k - T_a) \quad (3)$$

where $h_1=h(p_e,T_1)$ and h_2 are the refrigerant specific enthalpies at the suction and discharge lines, respectively, W_k is the compression power, and T_k is the average compressor shell temperature assumed to be equal to the compressor discharge temperature, $T_k \approx T(p_c,h_2)$. Hermes and Melo (2008) showed that UA_k is ruled by the refrigerant mass flow rate inside the compressor shell, which is very sensitive to the evaporating pressure. Since this parameter is not expected to vary significantly during the optimization exercise, UA_k was assumed to be constant. One should note that these assumptions do not affect the condenser energy balance significantly, as the heat transfer rate in the gascooling region is small in comparison to the heat transfer in the condensing region. In addition, it should be noted that the first term on the right hand side of eq. (3) is the net energy supplied to the refrigerant, whereas the second term is the heat lost to the surrounding air.

The refrigerant mass flow rate and the compression power were obtained from a semi-empirical model presented by Negrão et al. (2011). The former was calculated from:

$$m_r = (PD \cdot N / v_1)(a + b\, p_c / p_e) \quad (4)$$

where PD and N are the compressor displacement and angular speed, respectively, and $v_1=v(p_e,T_1)$ is the specific volume evaluated at the compressor inlet temperature. The second term between brackets refers to the actual volumetric efficiency, whereas the coefficients "a" and "b" were fitted to the manufacturer calorimeter data. The actual compression power was linearly fitted to the isentropic compression power, $W_k=W_u+m_r w_s/\eta$, where w_s is the isentropic compression work (Gosney, 1982), W_u is the power consumption for the compressor working unloaded, η is the thermodynamic efficiency of the compression process, being both fitted to the manufacturer calorimeter data.

2.4 Thermal Load and Energy Consumption

The cabinet thermal load, Q_t, is defined as the energy transferred from the surrounding environment to the refrigerator compartments in the form of heat and electrical power, as follows:

$$Q_t = UA_{fz}(T_a - T_{fz}) + UA_{ff}(T_a - T_{ff}) + W_{fan} \quad (5)$$

where T_{ff} and T_{fz} are the average temperatures inside the fresh and frozen-food compartments, respectively, and W_{fan} is the power dissipated by the fan within the refrigerated cabinet. As the convective thermal resistances inside and outside the cabinet are small in comparison to the insulation counterpart, they were both disregarded so that the cabinet conductances were calculated from $UA=k_wA_w/l_w$, where k_w is the thermal conductivity of the insulated walls, l_w is the insulation thickness, and A_w is the external heat transfer area of each refrigerated compartment. It should be noted that the heat transferred through the gasket region, which often amounts ~10% of the thermal load, is embedded into the UA-coefficients.

As proposed by Hermes et al. (2009), the energy consumption of a thermostat-controlled refrigeration system can be calculated from:

$$EC = (W_k + W_{fan})(Q_t - W_{fan})/(Q_e - W_{fan}) \quad (6)$$

where $(Q_t-W_{fan})/(Q_e-W_{fan})$ is the compressor runtime ratio calculated according to an overall heat balance over a compressor cycle. It is worthy of mention that the average compression power, thermal load and cooling capacity were approximated by the steady-state values supplied by the model. Notably, eq. (6) has provided a good prediction for the energy consumption, as demonstrated in other studies (Hermes et al., 2009; Negrão and Melo, 2011; Hermes et al., 2012). The evaporator fan power, W_{fan}, is calculated as a function of the evaporator air flow rate according to 3rd degree power law approach $W_{fan}/W_{fan,0}=(m_{air}/m_{air,0})^3$, where the reference values of the evaporator fan power and air flow rate, indicated by the subscript "0", were obtained from experimental test data.

2.5 Solution Algorithm

The model was implemented into the EES platform (Klein, 2011) which solves the equation set simultaneously through the Newton-Raphson technique. All required thermodynamic and thermophysical properties were calculated using the REFPROP7 software (Lemmon et al., 2002).

3. MODEL VALIDATION

The refrigerator was originally tested by Hermes and Melo (2008). The refrigerator was instrumented with 60 thermocouples, 2 pressure transducers, one of them positioned at the compressor suction line and the other at the discharge line, and 2 power analyzers to record the energy consumed by the compressor and fan separately. The tests were conducted at an ambient temperature of 32°C. Steady-state tests were performed in order to determine the thermal conductances and the air flow rate in each refrigerated compartment. The latter was performed using a wind-tunnel facility, whereas the former was carried out with the refrigerator placed in a controlled temperature and humidity chamber.

Transient energy consumption tests were also conducted with the refrigerator controls (a thermostat driven by the frozen-food compartment temperature, and a thermostatic damper driven by the fresh-food compartment temperature) set to their maximum and minimum cooling capacities, so that a dataset comprised by four data points was obtained (thermostat-damper): Min-Min, Min-Max, Max-Min, Max-Max. The product was instrumented according to the recommendations of ISO 8561 (1995) standard.

First, the compressor model equations were best fitted to experimental data obtained from the compressor maps. Three other compressors with HFC-134a as working fluid were additionally used: (i) a single-speed one with a higher COP and the same piston displacement, (ii) another single-speed compressor with a larger piston displacement and the same COP, and (iii) a variable-speed compressor with the same piston displacement used in (ii). Table 1 shows the performance data of the compressors. A comparison between the model predictions and the experimental counterparts was performed for all compressors, when discrepancies within 9% and 5% error bands were found for the power consumption and mass flow rate, respectively, as shown in Fig. 2.

Table 1: Performance data for the four compressors under analysis

Compressor Model	PD [cm³]	COP* [-]
Original (OR)	7.15	1.47
High Efficiency (HE)	7.15	1.72
Large Displacement (LD)	7.95	1.47
Variable Capacity (VSC)	7.95	1.67**

* At the rating point condition (-23.3°C/54.4°C, ASHRAE S23, 1993). ** At 3600 rpm.

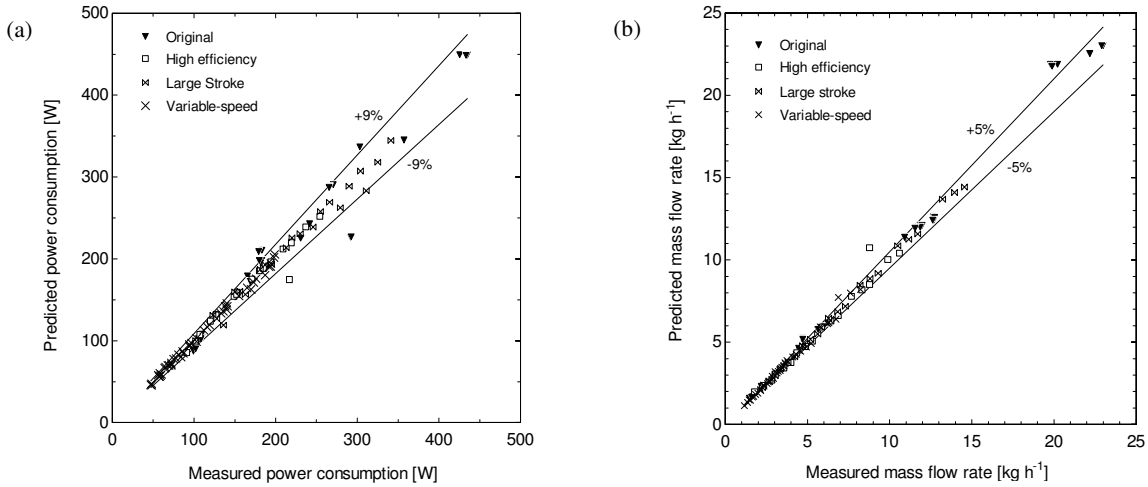

Figure 2: Compressor model validation for all compressors: (a) compression power, and (b) mass flow rate

The conductances (UA) of the fresh and frozen-food compartments were calculated by Hermes and Melo (2008), who reported UA_{ff}=1.516 and UA_{fz}=0.523 W/K. The condenser conductance, UA_c, was calculated from the correlation of Melo and Hermes (2009), and the evaporator conductance, UA_e, was calculated from the correlation of Barbosa et al. (2009), with a scaling factor α required to adjust the correlation (obtained for evaporators with slit fins) to the evaporator under analysis (which employs continuous flat fins). The compressor conductance, UA_k, and the α-factor were best fitted to energy consumption data in order to minimize the root mean square (RMS) difference between calculated and measured values of evaporating and condensing pressures, compressor shell temperature, energy consumption and runtime ratio, resulting in UA_k=2.28 W/K and α=0.7. For the remaining empirical parameters, the average values observed during the energy consumption tests were adopted, i.e. ε=0.8, ϕ=0.8, $m_{air,0}$=64 kg/h, $W_{fan,0}$=7 W, ΔT_{sh}=5 K and ΔT_{sc}=1 K.

The simulation model also needs to be fed with compartment (5°C and -18°C) and surrounding (32°C) air conditions, the condenser and evaporator geometries (90 wires and 27 fins), and the insulation thicknesses of both the frozen and fresh-food compartments (l_{ff}=47 mm and l_{fz}=65 mm). Table 2 summarizes the model validation exercise, where it can be seen that the system simulation model is able to predict the overall energy consumption, compression power and runtime ratio within a ±9% error band.

Table 2. Comparison between calculated and measured energy consumption, compression power and runtime ratio

	Energy consumption [kWh/month]			Compression Power [W]			Runtime ratio [-]		
Condition	Calculated	Measured	Diff.	Calculated	Measured	Diff.	Calculated	Measured	Diff.
Min-Min	44.55	44.11	1.0%	145.2	137.6	5.2%	0.407	0.427	-5.0%
Min-Max	52.33	51.42	1.7%	140.3	137.3	2.1%	0.493	0.502	-1.7%
Max-Min	48.96	53.24	-8.7%	122.8	125.2	-2.0%	0.524	0.560	-6.9%
Max-Max	58.74	62.61	-6.6%	121.1	124.2	-2.6%	0.637	0.667	-4.7%

4. OPTIMIZATION SCHEME

The optimization work was carried out with the focus on both energy and cost savings. However, one should bear in mind that energy and cost are tradeoff design criteria, so as to reduce the first the second must increase. In order to

take it into account, the optimization task was performed to minimize the energy consumption with the total system cost fixed. In such case, the evaporator air flow rate, the number of evaporator fins and condenser wires, and both frozen and fresh-food compartment thicknesses were considered independent variables. Despite the system cost was held constrained, the individual component costs can vary freely. It should be additionally noted that the cabinet envelope is held constrained thus ensuring that the appliance fits in the space available in customer's kitchens. Therefore, for a fixed envelope, extra insulation thickness implies in a lower internal volume, which may affect not only the declared energy consumption for the sake of labeling purposes, but also the cabinet volume class.

The total system cost is calculated as the sum of the evaporator, condenser, insulation and compressor costs. The evaporator and condenser costs were computed as a function of the heat transfer surface area, the cabinet insulation costs were expressed in terms of the insulating thicknesses, and the compressor cost was estimated according to its nominal performance (COP) and size (piston displacement, PD). The final cost function is as follows:

$$C_t = c_{ff} l_{ff} + c_{fz} l_{fz} + c_c A_c + c_e A_e + c_k COP^{3/4} PD^{1/3} \quad (7)$$

where c_{ff}=230 \$/m and c_{fz}=135 \$/m are the unitary costs per thickness length of the fresh and frozen-food compartment thicknesses, respectively, l_{ff} and l_{fz} are the insulation thickness of the fresh and frozen-food compartments, respectively, A is the heat transfer surface area, c_c=2 \$/m^2 and c_e=7 \$/m^2 are the unitary costs per area of the condenser and evaporator, respectively, c_k=10.1 \$/cm is the unitary cost of the single-speed compressors, COP is the compressor coefficient of performance at the ASHRAE S23 (1993) rating point condition (-23.3^{o}C/54.4^{o}C), and PD is the compressor displacement [cm^3].

It is worth noting that the cost structure depends not only on the commodities and transformation costs, but also on trading strategies, which are far beyond the scope of this study. The cost structure adopted in present work aimed uniquely at showing the capabilities of the proposed optimization methodology and, therefore, better results can be achieved if a more realistic cost structure is adopted. Nevertheless, it should be emphasized that the normalized cost structure was designed to reflect the real costs usually observed in frost-free refrigerators, which in the present study is as follows: 47% compressor, 3% condenser, 13% evaporator, and 37% insulation.

5. RESULTS

The optimization task was firstly carried out in order to come out with the geometric parameters (number of evaporator fins and condenser wires, and insulation thicknesses) and the air flow rate that minimize the energy consumption for a fixed cost. For this purpose, the built-in EES *genetic optimization algorithm* was employed (Klein, 2011). For an original system cost of \$53.5, a minimum energy consumption of 43.0 kWh/month was achieved for N_{wires}=58, N_{fins}=9, l_{ff}=61 mm, l_{fz}=78 mm, m_{air}=34 kg/h in case the compressor is not replaced. The cost was redistributed between the system components according to eq. (7), in such a way that the number of condenser wires and evaporator fins decreased by 36% and 67%, respectively, whereas the insulation thicknesses of the fresh and frozen-food compartments increased by 31% and 20%, respectively, thus indicating that the energy consumption showed to be more sensitive to cabinet insulation rather than to condenser and evaporator heat transfer area. In addition, once the cabinet envelope was held constrained, an increasing insulation thickness implies in a smaller internal volume. In the present optimization exercise, a cabinet volume reduction of 11.5% was observed.

Figure 3 shows the individual effects of the heat exchanger areas on both the energy consumption and cost in case when the remaining optimization variables (l_{ff}, l_{fz}, m_{air}) are fixed at their optimum values. One should note that while the overall cost is a linear function of the condenser and evaporator areas, the energy consumption describes a strongly non-linear behavior. The cost and energy consumption tradeoff is clearly depicted in Fig. 3, as the former increases and the latter decreases with the addition of either the condenser wires or evaporator fins. In addition, both energy consumption and cost are more sensitive to changes in the evaporator area in comparison with the condenser counterpart. The optimum values are obtained in Fig. 3 when a constant energy consumption curve is tangent to a constant cost curve (see the lines at the bottom left corner), where the minimum energy consumption is 17.7% lower than the baseline at no cost penalty. Moreover, it should be also noted that two optimization exercises can be performed in Fig. 3: one can be accomplished by following a constant energy consumption curve to reach the minimum cost line, and another by moving over a constant cost straight line towards the minimum energy consumption curve.

Figure 4 assesses the effect of the evaporator air flow rate on the energy consumption, whereas the other parameters are held fixed. It can be seen that the minimum energy consumption is found for the air flow rate of 34 kg/h, which is 6% lower than that observed for the baseline refrigerator (original components). One should note that, on one hand, an increasing air flow rate induces a higher evaporating temperature thus improving its performance, but, on the other hand, the fan pumping power also increases. Such a tradeoff explains the minimum observed in Fig. 4.

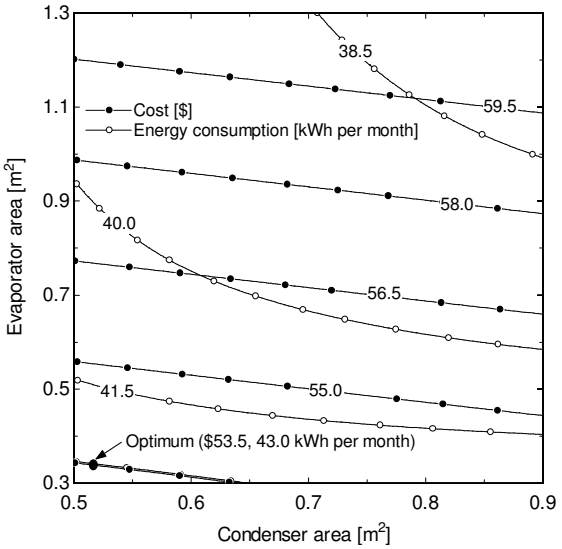

Figure 3: Effects of evaporator and condenser areas on both energy consumption and cost (original compressor)

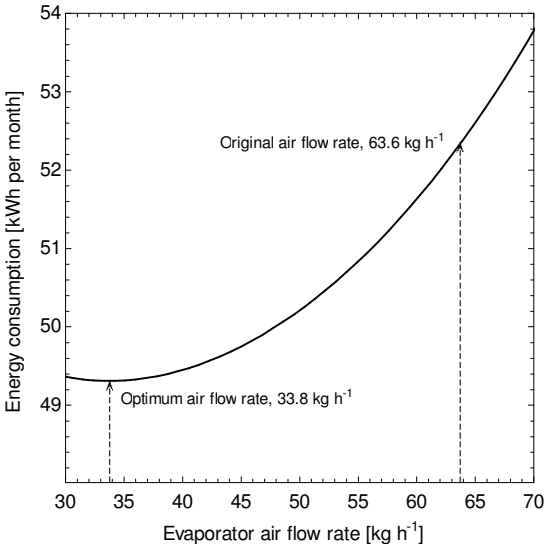

Figure 4: Effect of evaporator air flow rate on the energy consumption for the original system components

The effects of two different single-speed compressors available on the market on the system performance were also evaluated. In comparison to the original compressor (OR), the high efficiency (HE) one has a COP 17% higher and the same cooling capacity (at the rating point condition), while the large displacement (LD) one has a cooling capacity 11% higher with the same COP, as shown in Table 1. Simulations for the refrigerator working with each one of these compressors, but keeping the other components at their original configuration, were conducted and the resulting performances are presented in Table 3. One should note that the mere substitution of the original compressor by the HE and LD compressors reduced the system energy consumption in comparison to the baseline refrigerator in 16% and 2%, respectively, with cost increase of 6% and 1.6%, respectively. A previous investigation shows that the energy consumption is expected to diminish when the compressor is replaced by a lower displacement one (Hermes et al., 2009). However, a 2% energy consumption reduction was observed in case when the large displacement compressor was adopted. This is so as the large displacement compressor presents a higher COP in the system condition (evaporating and condensing temperatures) than the original compressor, although both compressors have the same COP at the check point condition.

Table 3: Comparison of the system performance for the single-speed compressors

Compressor	EC [kWh per month]	EC diff. [%]	Cost [$]	Cost diff. [%]
OR	52.3	-	53.5	-
HE	44.0	-16.0	56.8	6.0
LD	51.1	-2.3	54.4	1.6

Table 4 presents the cost and energy savings (in comparison to the baseline system) achieved after the optimization exercise for each one of the three single-speed compressors under analysis. A comparison between Tables 3 and 4 shows that replacing the original compressor by the HE one without any further component matching causes the system cost to increase by 6% while the energy consumption is reduced by 16%. However, if the compressor replacement is followed by a proper component matching exercise, an energy consumption reduction of 14.4% is achieved with no cost penalty. Anyway, the system optimization for the original compressor led to an energy reduction of 17.7% (higher cooling capacity, lower compressor runtime), thus being preferable to the HE one.

Table 4: Energy and cost savings for the single-speed compressors

Compressor	Energy savings, %	Cost savings, %
OR	17.7	-
HE	14.4	5.5
LD	11.5	4.9

Figure 5 shows the minimum energy consumption as a function of the total system cost for all single-speed compressors under analysis. One should note that the values above the curve are not optima, case of the baseline system marked with a diamond, whereas the values below the curve do not fulfill the system constraints. As expected, the minimum energy consumption decreases with an increasing cost, and for lower energy consumption values (EC<35 kWh per month, where the OR and HE curves cross each other) the system cost is lower when the high efficiency compressor (HE) is employed. On the other hand, the use of a high capacity compressor (LD) is only feasible if the energy consumption target is relaxed (EC>55 kWh per month) leading to a poor system design in terms of energy performance. This is so because of runtime restrictions (<100%) that prevent the OR and HE compressor curves from reaching values of EC higher than 47 and 54 kWh/month, respectively. The replacement of the original compressor by the costly HE saves insulation material, thus allowing a cost reduction of 5.5% for the same energy target (see Table 4), which shows the cost savings attained when the energy consumption is constrained. Cost savings are not reported for the original compressor because of runtime restrictions.

The performance of a variable-speed compressor (VSC) is now evaluated comparing its optimum curves to that obtained by adopting the LD compressor as a reference (as it has the same displacement as the VSC compressor under analysis, as indicated in Table 1). Two optimum curves are plotted in Fig. 6 for the VSC compressor considering a cost scaling factor β, so that $C_{k,VSC}=\beta C_{k,LD}$, thus indicating how much the variable-speed compressor cost can be increased until it gets economically unfeasible. Energy consumption optimizations were carried out considering different β-values with the runtime ratio fixed at 100%, so that two curves were identified: the one that crosses the point of minimum energy consumption for the original cost (β=1.26), and the other one that crosses the point of minimum cost and original energy consumption (β=1.20), thus providing the optimization limits for the optimized refrigerator operating with the LD compressor. This result shows that in case the optimization is aimed at energy savings, the variable-speed compressor shall not cost 26% more than a single-speed compressor with the same piston displacement, otherwise it is not economically feasible. Similarly, in case the design is aimed at cost savings, the adoption of a variable-speed compressor is economically feasible only if its overall cost does not surpass 20% of that observed for a single-speed compressor with the same displacement. Of course, these results are restricted to the cost function adopted in this study.

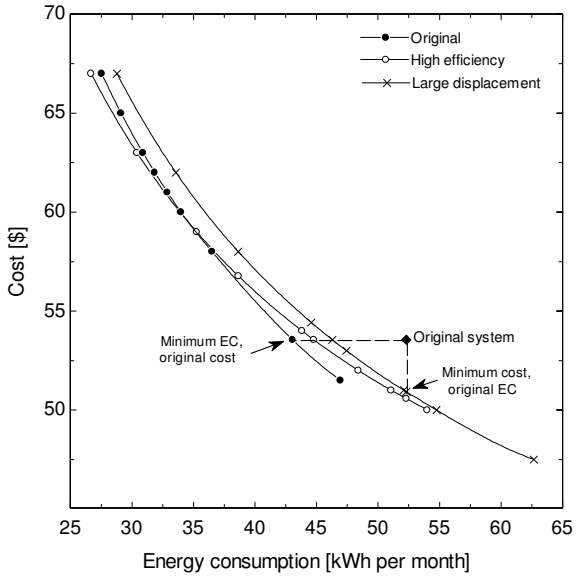

Figure 5: Optimized energy consumption and cost for the single-speed compressors

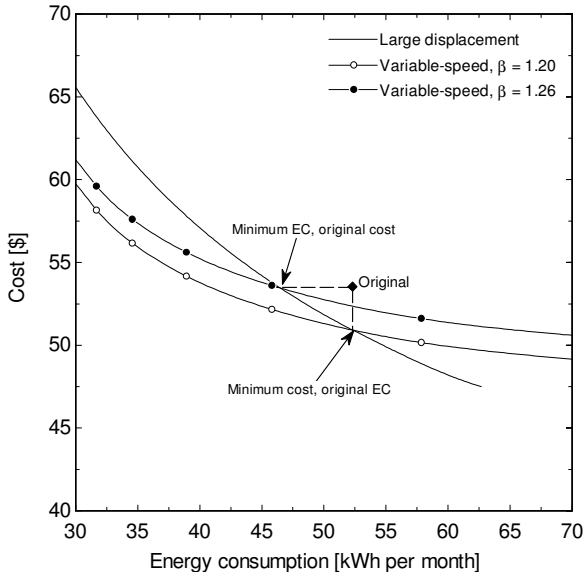

Figure 6: Optimized energy consumption and cost for the variable-speed compressor

6. FINAL REMARKS

A thermoeconomic design methodology for frost-free refrigerators with two compartments was presented. A simulation model was put forward, and its results were validated against experimental data, with predictions for energy consumption, compression power and runtime ratio agreeing with the experimental data within a ±9% error band. The model was used to optimize the refrigerator aimed at both energy consumption and cost savings based on the condenser and evaporator heat transfer surface, the air flow rate supplied to the evaporator coil, and the insulation thicknesses of the refrigerated compartments. The system optimization resulted in energy savings of 17.7% in comparison with the baseline refrigerator with no cost penalty. The proposed design algorithm resized the components – the evaporator and condenser areas were reduced while the cabinet insulation was increased – without changing the overall system cost. It was observed that the mere replacement of the original compressor by another with a COP 17% higher caused an energy consumption reduction of 16% followed by a cost increase of 5.5%. However, after an optimum component matching exercise, the figures changed to energy savings of 14.4% showing that the original compressor is preferable to the high efficiency one when the cost is constrained. However, it was found that the system working with the high COP compressor becomes more efficient when low energy consumption targets are aimed for.

The analysis also showed that in case the optimization is focused on energy savings, the variable-speed compressor shall not cost 26% more than a single-speed compressor with the same piston displacement, otherwise the new system design is not economically feasible. If the optimization is aimed at cost savings, a variable-speed compressor is feasible only if its overall cost does not surpass 20% of that observed for a single-speed compressor with the same displacement. Of course, such a conclusion applies to the refrigerator under analysis only. The cost analysis employed in this paper was estimated by the authors based on their prior experience with design and analysis of frost-free refrigerators and also on information available in the open literature. The proposed cost structure aimed uniquely at demonstrating the potentials of the proposed design methodology and might present deviations from actual industrial costs. More accurate optimization results can be obtained if a refined cost structure is provided.

NOMENCLATURE

A	heat transfer surface area, m^2
C	cost, $
c	unitary cost
c_p	specific heat at constant pressure, J kg^{-1} K^{-1}
COP	compressor COP at the rating condition
EC	energy consumption, kWh/month
h	specific enthalpy, J kg^{-1}
k	thermal conductivity, W $m^{-1}K^{-1}$
l	insulation thickness, m
m	mass flow rate, kg s^{-1}
N	compressor speed, s^{-1}
p	pressure, Pa
PD	compressor piston displacement, cm^3
Q	heat transfer rate, W
T	temperature, K
U	overall heat transfer coefficient, W $m^{-2}K^{-1}$
UA	thermal conductance, W K^{-1}
v	specific volume, m^3 kg^{-1}
W	power consumption, W
w_s	specific isentropic compression work, J kg^{-1}
W_u	unloaded compression power, W

Greek

ε	heat exchanger effectiveness
η	compression efficiency
ϕ	air flow fraction to the freezer

Subscripts

a	surrounding ambient
c	condenser, condensing condition
e	evaporator, evaporating condition
ff	fresh-food compartment
fz	frozen-food (freezer) compartment
k	compressor
m	air at evaporator inlet
r	refrigerant side
ref	reference value
sat	saturation
sc	subcooling degree
sh	superheating degree
st	saturation condition
t	total
w	cabinet insulation

REFERENCES

ASHRAE Standard S23, 1993, *Methods of testing rating positive displacement refrigerant compressor and condensing units*, American Society of Heating, Refrigerating and Air Conditioning Engineers, Atlanta-GA, USA

Bansal PK, Chin TC, 2003, Modelling and optimization of wire-and-tube condenser, *International Journal of Refrigeration* 26, 601-613

Barbosa Jr. JR, Melo C, Hermes CJL, Waltrich PJ, 2009, A Study of the Air-Side Heat Transfer and Pressure Drop Characteristics of Tube-Fin "No-Frost" Evaporators, *Applied Energy* 86, 1484-1491

Borges BN, Hermes CJL, Goncalves JM, Melo C, 2011, Transient Simulation of Household Refrigerators: A Semi-Empirical Quasi-Steady Approach, *Applied Energy* 88, 748-754

Gholap AK, Khan JA, 2007, Design and multi-objective optimization of heat exchangers for refrigerators, Applied *Energy* 84, 1226-1239

Gonçalves JM, Melo C, Hermes CJL, 2009, A semi-empirical model for steady-state simulation of household refrigerators, *Applied Thermal Engineering* 29, 1622-1630

Gosney WC, 1982, *Principles of Refrigeration*, Cambridge University Press, UK

Hermes CJL, Melo C, 2008, A first-principles simulation model for the start-up and cycling transients of household refrigerators, *International Journal of Refrigeration* 31, 1341-1357

Hermes CJL, Melo C, Gonçalves JM, 2008, Modeling of non-adiabatic capillary tube flows: A simplified approach and comprehensive experimental validation, *International Journal of Refrigeration* 31, 1358-1367

Hermes CJL, Melo C, Knabben FT, 2012, Alternative Test Method to Assess the Energy Consumption of Frost-Free Household Refrigerating Appliances, *14th Int. Refrigeration and Air Conditioning Conference at Purdue*, West Lafayette-IN, USA, Paper 2101

Hermes CJL, Melo C, Knabben FT, Gonçalves JM, 2009, Prediction of the energy consumption of household refrigerators and freezers via steady-state simulation, *Applied Energy* 86, 1311-1319

ISO 8561, 1995, *Household frost-free refrigerating appliances – Refrigerators, refrigerator-freezers, frozen food storage cabinets and food freezers cooled by internal forced air circulation – Characteristics and test methods*, International Organisation for Standardisation, Geneva, Switzerland

Klein SA, 2011, *Engineering Equation Solver User's Manual*, F-Chart Software, Middleton-WI, USA

Lemmon EW, McLinden MO, Huber M.L., 2002, *NIST Reference fluids thermodynamic and transport properties* – REFPROP 7.0, Standard Reference Database 23, National Institute of Standards and Technology, Gaithersburg-MD, USA

Melo C, Hermes CJL, 2009, A heat transfer correlation for the natural draft wire-and-tube condensers, International Journal of Refrigeration, *International Journal of Refrigeration* 32, 546-555

Melo C, Silva LW, 2010, A perspective on energy savings in household refrigerators, *Sustainable Refrigeration and Heat Pump Technology Conference*, Stockholm, Sweden

Negrão COR, Erthal RH, Andrade DEV, Silva LW, 2011, A Semi-Empirical Model For The Unsteady-State Simulation of Reciprocating Compressors For Household Refrigeration Applications, *Applied Thermal Engineering* 31, 1114-1124

Negrao COR, Hermes CJL, 2011, Energy and cost savings in household refrigerating appliances: A simulation-based design approach, *Applied Energy* 88, 3051–3060

Rice CK, 1987, The effect of void fraction correlation and heat flux on refrigerant charge inventory predictions, *ASHRAE Transactions* 93, 341-367

Waltrich M, Hermes CJL, Melo C, 2011b, Simulation-based design and optimization of refrigeration cassettes, *Applied Energy* 88, 4756–4765

Waltrich PJ, Barbosa JR, Hermes CJL, 2011a, COP-based optimization of accelerated flow evaporators for household refrigeration applications, *Applied Thermal Engineering* 31 129-135

ACKNOWLEDGMENTS

Financial support from the CNPq and CAPES agencies, Government of Brazil, is duly acknowledged.